Phytopathology Research

RESEARCH

Open Access

Effect of silver nanochitosan on control of seed-borne pathogens and maintaining seed quality of wheat

Divya Chouhan[1], Poulami Dutta[2], Debojit Dutta[3], Ankita Dutta[4], Anoop Kumar[4], Palash Mandal[2], Chandrani Choudhuri[5] and Piyush Mathur[1*]

Abstract

Seeds, considered as the foundation of agriculture, are invaded by a broad spectrum of seed-borne pathogens. The current study aimed to control seed-borne fungal pathogens of wheat, *Aspergillus flavus* and *A. niger*, by using Ag^{+} nanochitosan (Ag-NC) for nano-priming of seeds and enhancing seed quality. Nanochitosan (NC) and Ag-NC were synthesized using the gelation method and characterized by UV–vis spectrophotometry, FESEM, EDXS, and HRTEM. NC and Ag-NC showed irregular surface topography with an average particle size of 275 and 325 nm, respectively. Antifungal activity of both the nanoparticles at 0.1, 0.2, 0.3, 0.4, and 0.5 mg/mL revealed that Ag-NC at 0.5 mg/mL has completely terminated the mycelial growth of both pathogens. Malonaldehyde content increased to 77.77% in *A. flavus* and 82.66% in *A. niger* when exposed to 0.5 mg/mL Ag-NC. High-intensity fluorescence due to oxidative stress was observed in Ag-NC-treated pathogens. Ultra-structural changes in Ag-NC treated pathogenic spores under SEM displayed pronounced membrane damages. Wheat seeds were nano-primed with NC and Ag-NC at 0.5 mg/mL, and fungal load was examined to evaluate the mitigation of pathogenic stress and its effect on seedling growth promotion activity. Ag-NC priming reduced the fungal load and allowed successful seed germination. Ag-NC priming increased the albumin, gliadin, gluten, and glutenin content along with total phenol, reducing sugar and starch levels. Ag-NC priming increased the overall protein levels traced through SDS-PAGE. Seed priming with Ag-NC promotes seed germination, mean germination time, stress tolerance index, vigour, etc. NC and Ag-NC at 0.5 mg/mL showed no cytotoxic effect on the Human Embryonic Kidney (HEK293) cell line that ensures the nanoparticles are non-toxic. Thus, the synthesized nanoparticles exhibit a dual role in antifungal activity and plant growth promotion.

Keywords Antifungal efficacy, Nano-technology, Pathogenic stress, Ag^{+} nanochitosan, Wheat

Background

Wheat (*Triticum aestivum* L.), one of the most important cereal crops, is served globally as an essential staple food. It rates the highest grain production in comparison to other crops (Khan et al. 2023). In addition to mankind, wheat is also an important animal feed. However, the decrease in the global production rate is of greatest concern to agro-researchers and farmers (Majumder et al. 2013; Islam et al. 2015). The most vital input of agriculture is the seed, which has also been considered a direct mean of conveying seed-borne pathogens over the years.

*Correspondence:
Piyush Mathur
piyushmathur110@gmail.com; piyushmathur316@nbu.ac.in
[1] Microbiology Laboratory, Department of Botany, University of North Bengal, Darjeeling WB-734013, India
[2] Nanobiology and Phytotherapy Laboratory, Department of Botany, University of North Bengal, Darjeeling WB-734013, India
[3] Genetics and Molecular Biology Laboratory, Department of Zoology, University of North Bengal, Darjeeling WB-734013, India
[4] ANMOL Laboratory, Department of Biotechnology, University of North Bengal, Darjeeling WB-734013, India
[5] North Bengal St. Xavier's College, Jalpaiguri WB-735134, India

Disease caused by seed-borne pathogens acutely affects plant health and are liable to deteriorate the seed quality during storage (Majumder et al. 2013). Wheat seeds are known to be distressed by a large number of seed-borne pathogens, including *Aspergillus flavus*, *A. niger*, *Alternaria alternata*, *Fusarium graminearum*, *Curvularia lunata*, *Bipolaris sorokinaina*, *Helminthosporium sativum*, and *Penicillium chrysogenum* (Rehman et al. 2011; Majumder et al. 2013; Hussain et al. 2013; Raza et al. 2014; Mehboob et al. 2015). Sheltering these seed-borne pathogens inside wheat deteriorates plant morphological development and yield when sown in the field. Seeds are often attacked by bacteria, nematodes, and rodents due to unhygienic and unscientific storage conditions (Sarwar 2015; Ali et al. 2019). Amid of all the seed-borne pathogens, diseases caused by fungal pathogens suffer 60% economic loss worldwide (Majumder et al. 2013). Seed quality and its longevity are awfully hampered by the invasion of fungal pathogens during both pre-harvest and post-harvest periods (Martin et al. 2022). Seed-borne pathogens are reported to lower the amount of reducing sugar, protein, phenolics, and amino acids in seeds (Rao et al. 2014; Tahmasebi et al. 2023). Thus, the management of seed-borne pathogens is crucial for diminishing the loss of seed quality.

Various methodologies for administrating seed-borne pathogens with techniques, such as seed priming, seed treatment or seed dressing, use of fungicides and botanicals, have been studied in recent years (Islam et al. 2015). Despite using these strategies, the success rate for combating seed-borne pathogens has not been satisfactory recently (Martin et al. 2022; Khan et al. 2023). Seed treatment with synthetic fungicides like captan (heterocyclic nitrogen), farmerzeb (zinc salt), mancozeb (ethylene bis-dithiocarbamic acid), baytan (tridimenol), and thiram (dithiocarbamate) are often observed to increase the viability of seeds (Kadegea and Lyimo 2015). But tremendous use of chemical-derived fungicides leads to the lowering of seed health, followed by disturbing the soil mycoflora, arresting seedlings' nutritional qualities, and disrupting nitrification and denitrification processes (Choudhary 2018).

In that regard, the appraisal of an eco-friendly, perishable biomolecule like chitosan and its nanometal-derivatives are highly recommended by the scientific sphere. Several scientific groups have already confirmed metal-derived nanoparticles' antifungal efficacy, viz. Ag, Fe, Zn, Cu, Ni, etc. (Eskikaya et al. 2023). Applying metallic nanoparticles on pathogenic microbes is known to produce reactive oxygen species (ROS), inducing cellular damages and hampering their protein and nucleic acid (Dananjaya et al. 2017; Nguyen et al. 2023). In order to synthesize a beneficial and cost-effective metallic nanoparticle, the choice of metal is a stiff task. One needs to consider increased bioactivity, which has a low cost value and a threshold limit of metal exposure to the seeds before synthesizing any metallic nanoparticle.

Researchers have recently designed various multifaceted bio-derived molecules, such as nanoparticles or nanoconjugates to combat a broad spectrum of seed-borne pathogens (Banerjee et al. 2021). A number of researchers have introduced chitosan for synthesizing nanoparticles and its conjugates in view of the fact that chitosan is a biodegradable, biocompatible, less toxic, and cost-effective molecule (Hans and Lowman 2002; Sarkar and Acharya 2020). Scientists have so far confirmed the potentiality of chitosan as an optimistic antifungal agent bearing a polycationic nature, which allows the molecule to bind with negatively charged cell components of fungal pathogens (Sathiyabama and Charles 2015; Malerba and Cerana 2016; Sathiyabama and Parthasarathy 2016). Alteration of bulk chitosan into chitosan nanoparticles increases its bioactivity as an antifungal compound, permitting greater permeability into biological membranes, and increased encapsulation efficiency with larger surface area coverage and small particle size (Kong et al. 2010). Besides nanochitosan (NC), scientists have specialized focused on establishing metal conjugates of NC through ionic gelation, emulsification, precipitation, etc. (Antonoglou et al. 2018; Yanat and Schroen 2021). Various reports suggest that, with respect to chitosan and its nanoparticles, metal variants of chitosan nanoparticles are more efficient with raised biological activity, including antifungal effect. This increase in activity is due to structural and functional aspects that have changed, with more cationic groups, the involvement of active functional groups, and the increase in condensing capacity (Yanat and Schroen 2021).

The metal Ag^+ manifests various congestions against plant pathogens and can be used with absolute safety for the governance of plant pathogens compared to commercial fungicides (Sharma et al. 2018). When applied, nanoparticles consisting of Ag^+ ion boost the plants' physiology by enhancing the germination rate, delaying leaf senescence, increasing biomass, and strengthening the plant immune system (Mahakham et al. 2017; Sadak et al. 2019). Ag^+ is an established wound healer and a well-known antiseptic having a highly reactive moiety that can invade pathogenic membranes (Nagaraja et al. 2023). However, exposure to Ag^+ beyond the threshold level may lead to phytotoxic outcomes on the morphological to molecular level in plants (Tripathi et al. 2017). Henceforth, Ag^+ chosen under the optimum dose for synthesizing a conjugative nanoparticle, including chitosan as the mother molecule, may hypothetically lead to increased bioactivity.

Ag^+ nanoparticle is an established anti-microbial compound against an indefinite number of crop pathogens (Kumari et al. 2017; Ibrahim et al. 2020; Manssor et al. 2021). Under in vitro conditions, several workers have already explored the antifungal efficacy of Ag-NC on various seed-borne phytopathogens (Kaur et al. 2012; Kaur et al. 2015; Wang et al. 2015). However, there are very few reports on the in vivo use of Ag-nanochitosan (Ag-NC) in defeating seed-borne pathogens and alleviation of pathogenic stress responses, particularly related to wheat. The use of Ag-NC for defeating seed-borne pathogens of wheat through solid matrix priming of wheat seeds is a novel approach to our study. Our objective is to focus on reducing the fungal load on stored wheat seeds by nano-priming approach so that the seeds can germinate into healthy seedlings after they are sown. Present research involves the synthesis of Ag-NC using very low exposure of Ag^+ and used the same for the control of seed-borne pathogens of wheat. Experiments were designed in a comparative account between NC and Ag-NC to better understand the promotional bioactivity of Ag-NC over NC. The fungicidal activity of Ag-NC against seed-borne pathogens from the vegetative to cellular level is explored. Since, chitosan is known to promote plant growth, this study also includes the assessment of germination parameters along with biochemical aspects of the nanoparticle-primed wheat seeds. Effect of nano-priming on the profile of storage proteins of seeds were analysed through SDS-PAGE. Moreover, the cytotoxicity of the synthesized nanoparticles was checked on the mammalian kidney HEK293 cell line to confirm that the applied dosimetry of Ag is under the threshold level and has no chance of exhibiting metal toxicity to plants, soil, and humans.

Results

Synthesis and characterization of NC and Ag-NC

The synthesis of NC was stipulated by the appearance of an apparent clear solution with an absorption peak in UV–vis spectrophotometer at 300 nm. While a brownish-coloured solution for Ag-NC hydrogel with an absorption peak at 405 nm for Ag-NC (Fig. 1a, b). High Resolution Transmission Electron Microscopy (HRTEM) inspection revealed an aggregative nature for NC, with irregular shape and average particle size ranging between 68 and 384 nm (measured by ImageJ Software). Whereas, Ag-NC particles are sized between 100–365 nm with a spherical layout (Fig. 1c, d). In Field Emission Scanning Electron Microscopy (FESEM) analysis, both NC and Ag-NC showed uneven, irregular surface topography with highly compact texture (Fig. 1e, f). Ag-NC showed embedded spherical-sized nanoparticles, agglomerated in masses. EDXS spectrum confirms the presence of Ag^+ in a very low proportion of only 1.14 atomic % of the total atomic weight of Ag-NC nanoparticle. Other necessary elements down to boron were also validated in the EDXS analysis (Fig. 1g, h).

Isolation of seed-borne pathogens from infected wheat seeds

The two high-frequency seed-borne pathogens were identified as *A. flavus* (ID 11,117.19) and *A. niger* (ID 11,531.21) that showed 45% and 32.5% fungal frequency from stored seeds of wheat. *Aspergillus* belonging to the phylum Ascomycota is a filamentous fungi having conidiophores that bear a chain of conidia attached to a club-shaped sterigmata, as observed under a microscope, *A. flavus* and *A. niger* (Additional file 1: Figure S1).

Effect of NC and Ag-NC on mycelium radial growth, lipid peroxidation, ROS production, and ultra-structural changes in major seed-borne pathogens *A. flavus* and *A. niger*

The assessment of the fungicidal activity of the synthesized NC and Ag-NC was evaluated by checking the mycelial growth of *A. flavus* and *A. niger* under a gradient of concentrations of the nanoparticles in vitro. The antifungal efficacy of NC and Ag-NC was estimated by measuring the colony diameter of both the seed-borne pathogens grown in PDA treated with 0.1, 0.2, 0.3, 0.4, and 0.5 mg/mL concentrations of both nanoparticles. The radial mycelial growth of *A. flavus* and *A. niger* was observed to be decreased with the rise in the concentration of the nanoparticles (Fig. 2a). After seven days post-incubation, the control plates showed a colony diameter of 9 cm and 8.7 cm for *A. flavus* and *A. niger*, respectively. Colony diameter of both pathogens was reduced successively with the hike in the concentration of nanoparticles. At 0.5 mg/mL, NC-treated plates for *A. flavus* showed 7.1 cm of colony diameter, equating to only 22.3% of Percent inhibition of radial growth (PIRG), and for *A. niger*, claiming 59.12% inhibition, showing 3.2 cm colony diameter (Fig. 2b, c). While plates treated with 0.5 mg/mL of Ag-NC exhibited complete termination of fungal growth, leading to 100% PIRG of both pathogens (Fig. 2c). Aqueous solution of $AgNO_3$ was served as positive control, and it was observed that individual effect of $AgNO_3$ against *A. flavus* and *A. niger* was lower in comparison to Ag-NC and NC against the same pathogens (Additional file 2: Figure S2).

A significantly higher level of Malonaldehyde (MDA) was generated with the increasing dosimetry of NC and Ag-NC. NC at 0.5 mg/mL showed 82.66% and 47.11% of MDA for *A. flavus* and *A. niger*, respectively (Fig. 3a). At the same aforesaid concentration, Ag-NC produces increased percentage of MDA in both the seed-borne

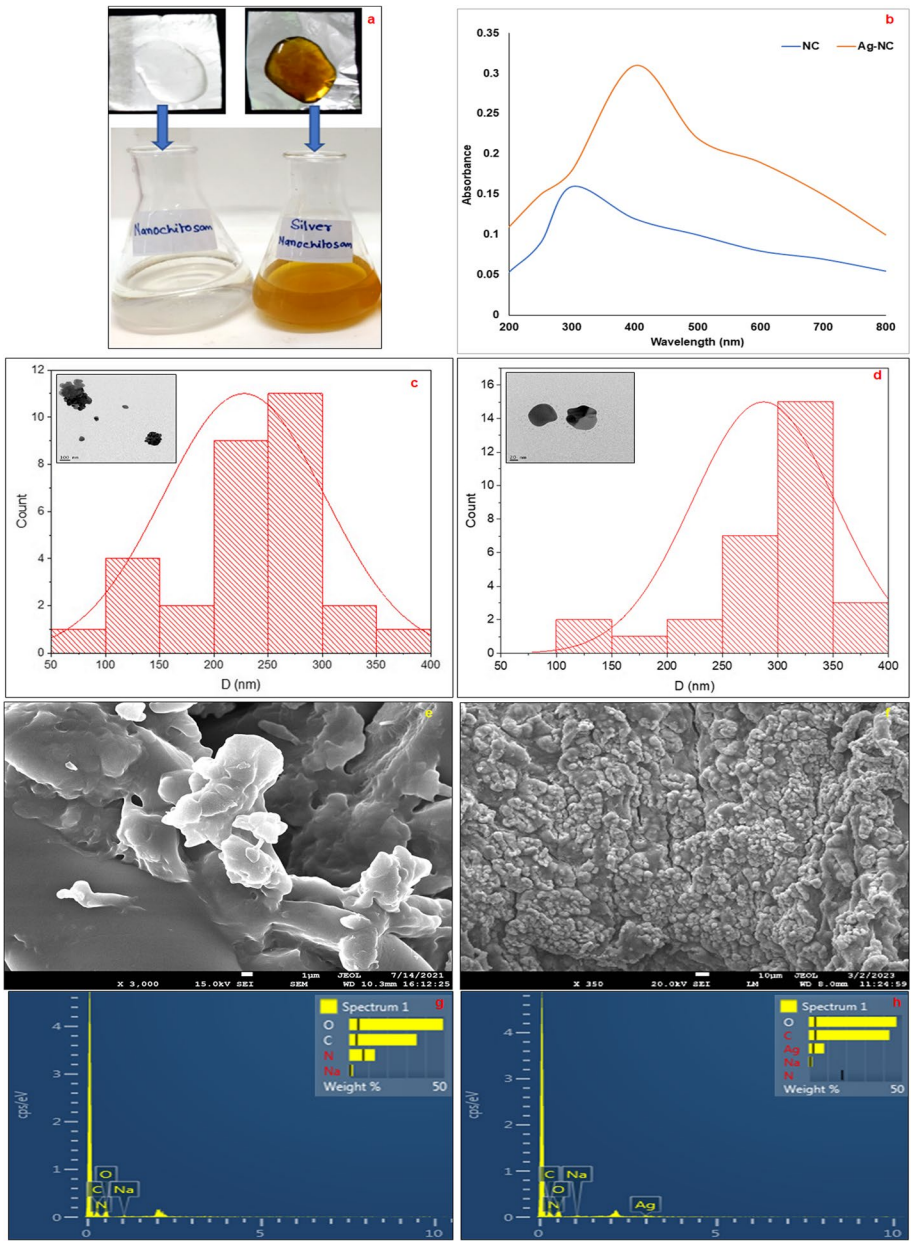

Fig. 1 **a** Synthesis of NC and Ag-NC through ionic gelation method; **b** The characterization on the basis of UV–vis spectral absorbance; **c** and **d** HRTEM analysis and particle size distribution histogram of NC and Ag-NC; **e** and **f** FE-SEM analysis of NC and Ag-NC; **g** and **h** EDXS analysis of NC and Ag-NC

pathogens in comparison to NC. *A. flavus* gives rise to 77.77% of MDA as a result of the treatment of 0.5 mg/mL of Ag-NC, whereas, *A. niger* generates 83.16% of MDA at the maximum used concentration of the same (Fig. 3a).

The visualization of fluorescence through the Dichlorodihydro-fluorescein (DCFH) staining method further confirmed the generation of oxidative stress in *A. flavus* and *A. niger* after 72 h of nanoparticle treatment. Figure 3b–g represents fluorescence microscopic images related to the generation of oxidative stress in distilled water (control), NC (0.5 mg/mL), and Ag-NC (0.5 mg/mL) treated fungal mycelium and sporangium of both *A. flavus* (Fig. 3b–d) and *A. niger* (Fig. 3e–g). Distilled water-treated fungal mycelium showed no appearance of fluorescence. Mycelium given NC treatment shows moderate to weak intensity of fluorescence. In contrast, fungal mycelium treated with Ag-NC showed the generation of maximum intensity of fluorescence, demarcating high production of oxidative stress.

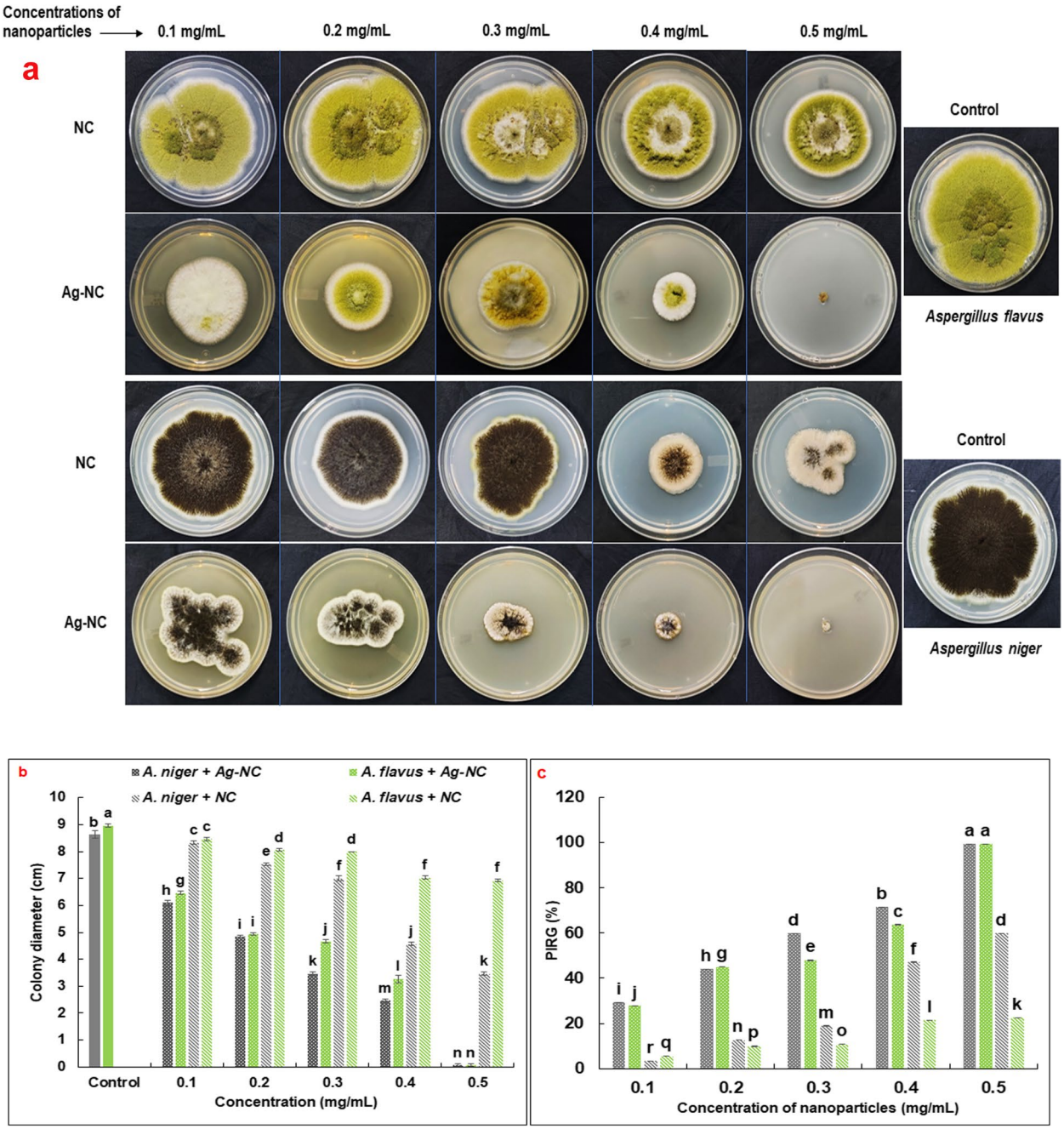

Fig. 2 **a** Effect of NC and Ag-NC on mycelium radial growth of *A. flavus* and *A. niger* with different concentrations (0.1, 0.2, 0.3, 0.4 and 0.5 mg/mL) of NC and Ag-NC on PDA plate. **b** Graphical representation of colony diameter of *A. flavus* and *A. niger* with different concentrations of NC and Ag-NC in comparison with control at 7 days post-incubation; **c** The percent inhibition of radial growth (PIRG) of *A. flavus* and *A. niger* under tested concentrations of NC and Ag-NC. Values are averages of three replicates ($n = 3$), error bars indicate standard deviation (SD) and different letters (a, b, c, etc.) indicate significant differences between treatments at $p \leq 0.05$ by Duncan's Multiple Range Test

Alterations in the morphology of the nanoparticles treated spores at the ultra-structural level were traced under Scanning Electron Microscopy (SEM) for both pathogens. Spores treated with distilled water (control) revealed no morphological deformities. Negligible structural abnormalities were noticed in NC (0.5 mg/mL) treated pathogenic spores. In contrast, spores influenced by Ag-NC (0.5 mg/mL) treatment exhibit pronounced disruptions in their membrane as observed in both the couple of pathogens. Severely damaged spore walls with

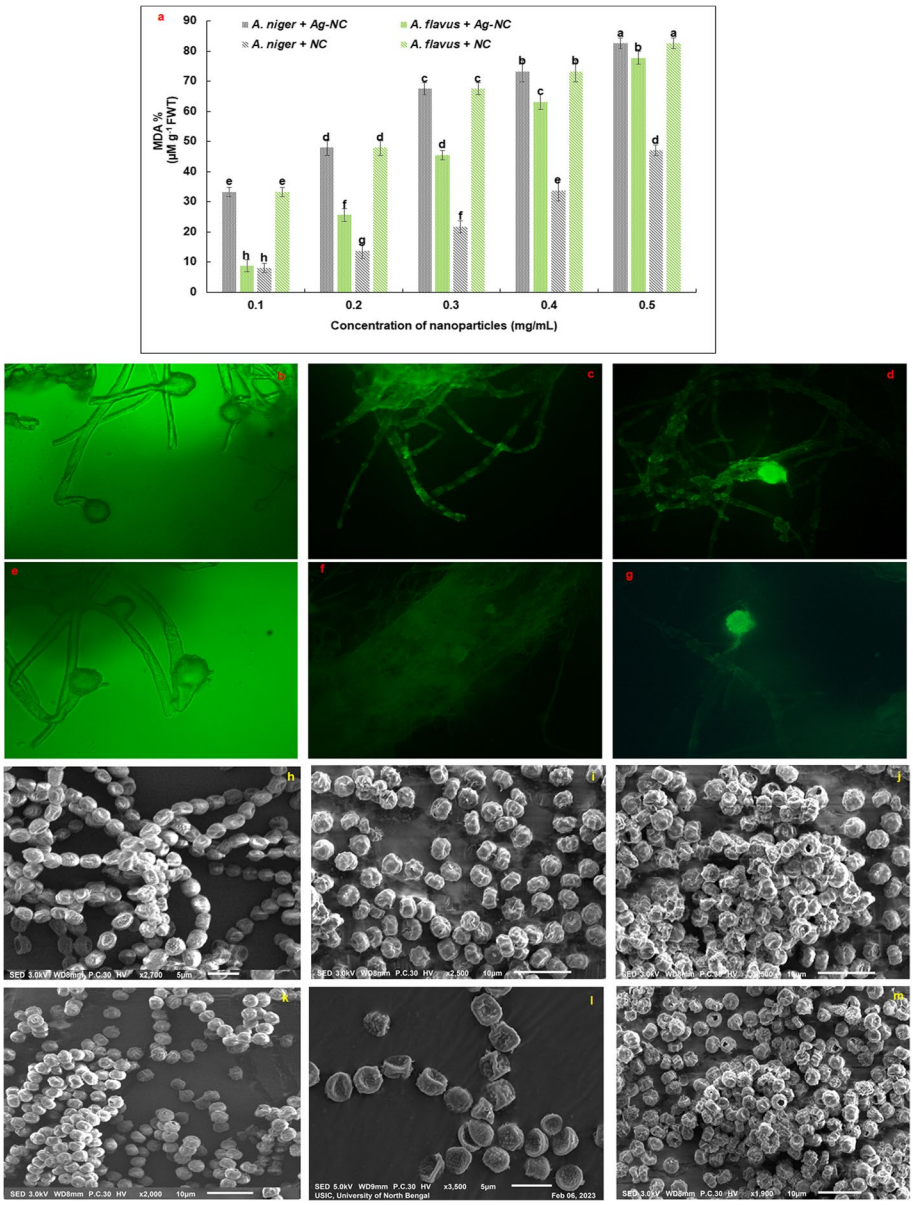

Fig. 3 **a** Effect of different concentrations of NC and Ag-NC on MDA percentage of *A. flavus* and *A. niger*. Fluorescence microscopic observations showing generation of oxidative stress in **b–d** *A. flavus* and **e–g** *A. niger* sporangium and mycelium due to the effect of **b**, **e** distilled water, **c**, **f** NC (0.5 mg/mL), and **d**, **g** Ag-NC (0.5 mg/mL); Morphological changes of *A. flavus* spores directly exposed to **h** distilled water, **i** NC (0.5 mg/mL), **j** Ag-NC (0.5 mg/mL); and *A. niger* spores treated with **k** distilled water, **l** NC (0.5 mg/mL) and **m** Ag-NC (0.5 mg/mL) observed under SEM. Data are represented as the averages of three replicates ($n = 3$), error bars indicate SD and a, b, c, etc.indicate significant differences between treatments at $p \leq 0.05$ by Duncan's Multiple Range Test

visible pores were also observed in Ag-NC feted *A. flavus* and *A. niger* spores. Aggregation of the fungal spores on masses was interestingly observed in Ag-NC treatment (Fig. 3h–m).

Fungal load in nano-primed wheat seeds

The effect of nano-priming with NC and Ag-NC on stored wheat seeds was checked to evaluate the mitigation of pathogenic stress generated by seed-borne pathogens on the seeds. Non-primed control seeds, when placed on PDA medium, liberated mycoflora harboured with seed-borne pathogens, which terminated the germination of the seeds (Fig. 4a). Similarly, seeds primed with NC (0.5 mg/mL) also remained ungerminated and liberated seed-borne mycoflora on the media (Fig. 4b). In contrast, seeds primed with Ag-NC (0.5 mg/mL) showed no

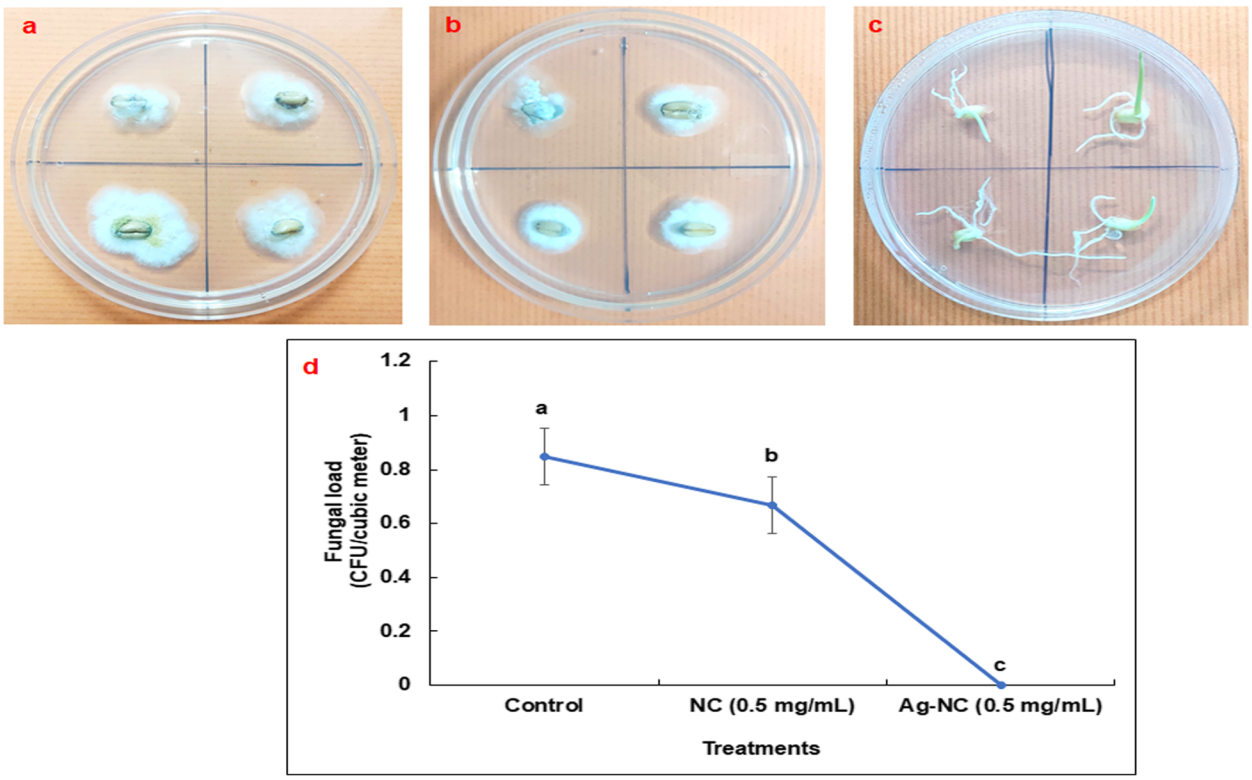

Fig. 4 Determination of fungal load in stored wheat seeds on 3rd day **a** non-primed, **b** NC (0.5 mg/mL), **c** Ag-NC (0.5 mg/mL); **d** Assessment of fungal load in treated wheat seeds. Values in the line graph are the average of three replicate plates ($n = 3$), error bars indicate SD and a, b, c, etc. indicate significant differences between treatments at $p \leq 0.05$ by Duncan's Multiple Range Test

liberation of any mycoflora in the media and successful germination of all the seeds placed on the plate (Fig. 4c). Statistically, the fungal load was found higher in non-primed seeds. NC priming in the seeds showed a reduction in fungal load by 21.42%, whereas Ag-NC priming showed a 100% reduction of fungal load in the seeds (Fig. 4d).

Effect of seed nano-priming on seed quality, germination, and disease incidence of wheat seeds

The effect of solid matrix priming with NC and Ag-NC on wheat seeds was evaluated by the estimation of essential biochemical parameters that affect seed quality. The albumin content in the non-primed seeds was traced to be 1.6 mg/g FWT, which increased by 2.75 folds in seeds primed with 0.5 mg/mL NC. Whereas the albumin content was significantly raised by 4.25 folds in seeds primed with 0.5 mg/mL Ag-NC. The globulin level in the NC primed seeds rose by more than 3 folds when compared to non-primed seeds. This level of globulin is again increased by 6.5 folds in seeds primed with Ag-NC. The gliadin content increased by 52.90% and 315% in NC and Ag-NC primed seeds, respectively, in comparison to non-primed seeds. Similarly, the gluten content rose by 4.64 folds in NC primed seeds and 5.78 folds in Ag-NC primed seeds when compared with the non-primed seeds (Fig. 5a). The phenol content in the non-primed seeds was estimated to be 1.23 µg/mg FWT which is found to be increased by 19% in NC primed seeds and by 40% in Ag-NC primed seeds (Fig. 5b). On the other hand, the reducing sugar content raised by 1.40 folds and 1.87 folds, respectively, in NC and Ag-NC primed seeds, with respect to non-primed seeds (Fig. 5c). The starch content in the NC primed seeds increased by 46.15% in comparison to non-primed seeds. This starch content increased by 126% in seeds primed with Ag-NC (Fig. 5d).

Analysis of the SDS banding pattern of NC and Ag-NC primed wheat seeds resulted in 14 major bands (Fig. 6a). The intensity of the band is significantly higher in Ag-NC primed seeds, which demarcates that the expression of a particular protein is quantitatively higher in seeds primed with Ag-NC (Fig. 6a). The integrated density of band at 63 kDa is increased by 20% in NC-primed seeds and by 44.39% in Ag-NC primed seeds, with respect to non-primed seeds (analyzed through ImageJ software) (Fig. 6b). Also, the integrated density of the band at 35 kDa is increased by 36.87% and 40.30% in NC and

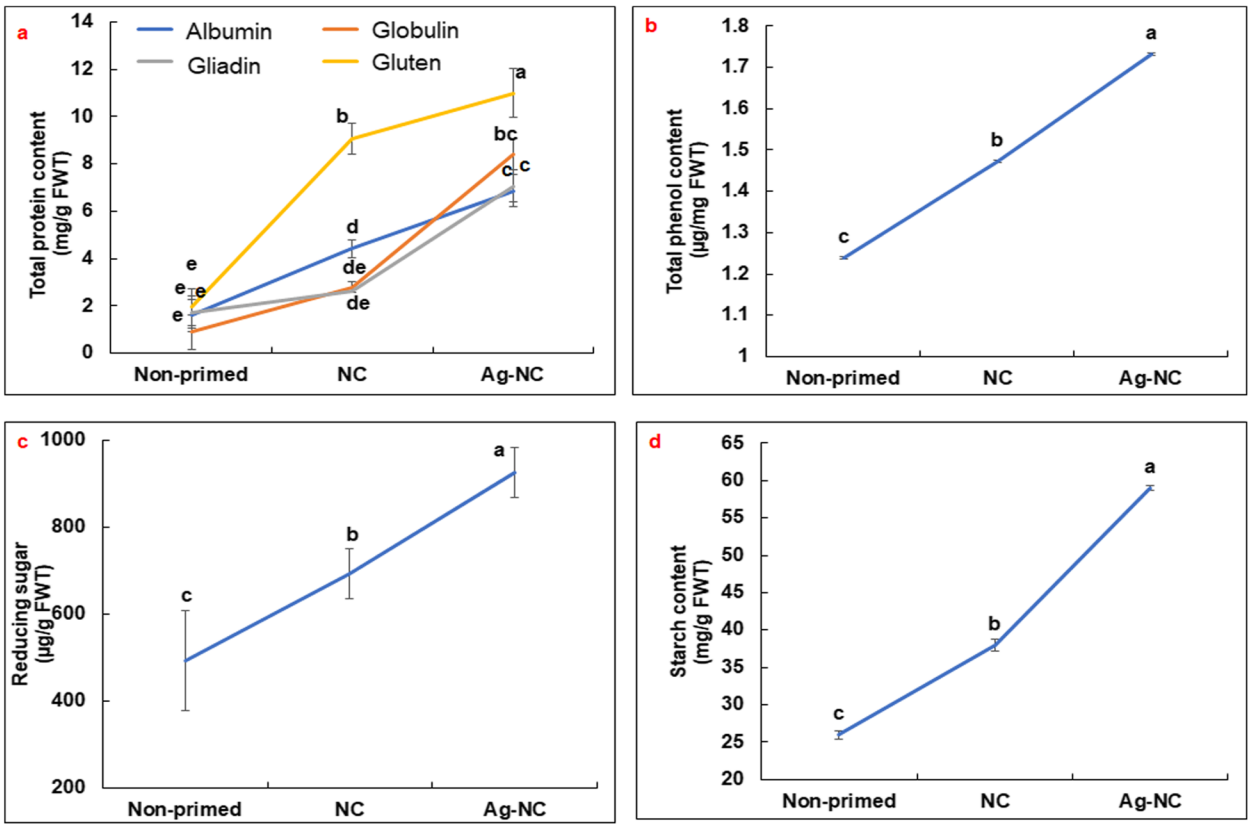

Fig. 5 Effect of solid matrix priming of wheat seeds on **a** total protein content, **b** total phenol content, **c** reducing sugar, and **d** starch content. Values are represented as the mean of three replicates ($n = 3$), error bars indicate SD and a, b, c, etc.indicate significant differences between treatments at $p \leq 0.05$ by Duncan's Multiple Range Test

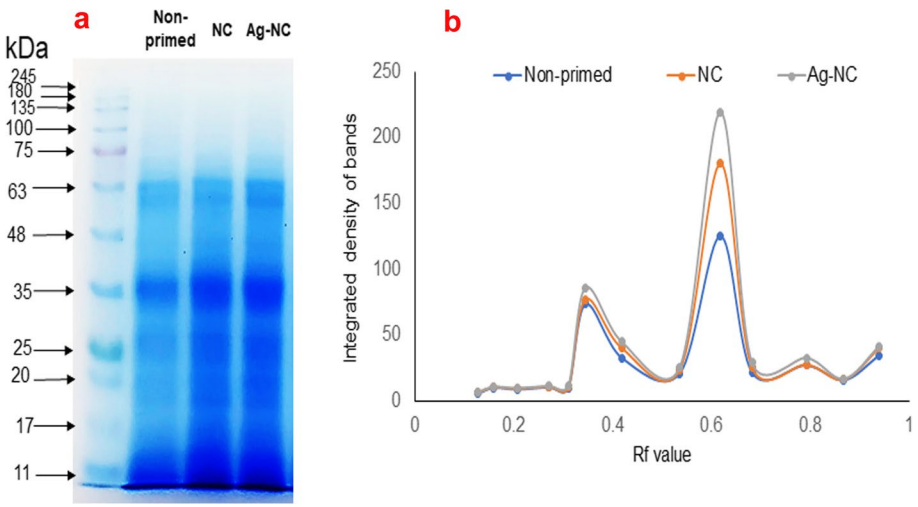

Fig. 6 Analysis of storage protein profiling through SDS-PAGE after nano-priming of stored wheat seeds. Non-primed seeds, NC (0.5 mg/mL) primed seeds, and Ag-NC (0.5 mg/mL) primed seeds

Ag-NC primed seeds, respectively, in comparison to non-primed seeds (Fig. 6b).

The effect of solid matrix priming with the synthesized nanoparticles on wheat seed physiology was examined through the evaluation of germination-related parameters (Table 1). Non-primed seeds given treatment with distilled water showed only 32% of seed germination (SG), whereas NC and Ag-NC primed seeds revealed 62% and 90% germination, respectively (Table 1). The MGT in NC-primed seeds decreased by 6.25% from the MGT in non-primed seeds. The MGT in Ag-NC primed seeds is further decreased by 9.27% in comparison to non-primed seeds (Table 1). Similarly, the GSTI of the seedlings whose seeds were primed with Ag-NC significantly increased to 200% with respect to non-primed (18%), where seeds were manifested with pathogens and without any priming (Table 1). PI was also found to be elevated by 4.88 folds in Ag-NC primed seeds and by 3.44 folds in NC primed seeds when contrasted with non-primed seeds (Table 1). Results of VI proclaimed that non-primed seeds germinated with retarded root-shoot length (500.23 unit), whereas NC priming resulted in increased VI by 50% and by 170% for seeds primed with Ag-NC as compared with non-primed seedlings (Table 1).

On the 7th day of germination, the NC and Ag-NC primed seeds revealed a significant difference in the reduction of disease incidence and promotion of germination parameters of the seedlings. The non-primed seeds showed significant establishment of disease in the seedlings, with 88.66% disease incidence, whereas NC primed seeds displayed 46.66% disease incidence. A remarkable reduction in the disease incidence was traced in the seedlings whose seeds were primed with Ag-NC, which showed only 10% disease incidence (Table 1).

Cytotoxicity of NC and Ag-NC

The cytotoxic effect of the synthesized nanoparticles was examined on the mammalian HEK293 cell line through an (3-[4,5-dimethylthiazol-2-yl]-2,5 diphenyl tetrazolium bromide) MTT assay. Mammalian cells were exposed to an increasing range of dosimetry, from 0.1–2 mg/mL of NC and Ag-NC. Results revealed that both the nanoparticles possess no cytotoxic effect on the seeded cells up to 1.4 mg/mL concentration. Cell proliferated successfully in the medium treated with 0.1–1.4 mg/mL of both NC and Ag-NC. But beyond 1.4 mg/mL of NC and Ag-NC, a cytotoxic effect was observed in the seeded cells leading to the loss of reproductive ability and further proliferation. Treatment of the cells above 1.4 mg/mL of NC showed up to 10% cytotoxic effect, whereas Ag-NC treatment showed 30% cytotoxicity up to 2 mg/mL dosage, with respect to the cells treated with distilled water imposing no toxicity (Additional file 3: Figure S3).

Discussion

Chitosan is counted as one of the most powerful chelating agents that are able to form complexes in the company of heavy metals and transition metals with ease (Jiang et al. 2011; Pivarciova et al. 2014; Pincus et al. 2021). Reports have stated that chitosan-involved metal complexes with transition metals (Ag, Cu, Fe, Ni, etc.) revealed enhanced antimicrobial properties in comparison to bulk chitosan because of the modifications in the physical structure of chitosan bearing -NH_2 and -OH group as predominant reactive sites (Wang et al. 2005; Ardean et al. 2021). Chitosan, with its nano-metal derivatives, exhibits a broad spectrum of antifungal properties against *Aspergillus niger*, *A. flavus*, *Alternaria solani*, *Fusarium oxysporum*, *Penicillium* spp., *Candida* spp., *Cordyceps militaris*, etc. (Qiang et al. 2011; Ilina et al. 2017; Liu et al. 2018). Therefore, chitosan has emerged as a key biodegradable molecule for the management of seed borne pathogens in food crops.

Ag^+ imparts deleterious reverberations on multiple pathogenic microorganisms along with the physiological upliftment of plants towards vigor. Ag^+ induces the resistance of plants to various diseases and abiotic stresses (Kale et al. 2021). An ion of this compassion, when impregnated with chitosan nanoparticles, hiked the antifungal activity along with plant developmental metabolism and stress resistance capacity (Anusuya and Banu, 2016; Santiago et al. 2019; Alghuthaymi et al. 2020). Our results demonstrated that Ag-NC could stand

Table 1 Effect of solid matrix priming of wheat seeds on seed germination (SG) %, mean germination time (MGT), germination stress tolerance index (GSTI), promptness index (PI), vigour index (VI), and disease incidence (DI) % of variably treated wheat seedlings at 7th day of germination

Treatment	SG %	MGT	GSTI	PI	VI	DI %
Non-primed	32 ± 1.84^{c}	95.97 ± 4.12^{a}	18 ± 4.20^{c}	18 ± 4.92^{c}	500.23 ± 10.05^{c}	88.66 ± 3.22^{c}
NC	62 ± 2.17^{b}	89.99 ± 4.45^{b}	187 ± 2.40^{b}	62 ± 3.31^{b}	750 ± 12.21^{b}	46.66 ± 1.09^{b}
Ag-NC	90 ± 1.72^{a}	86.23 ± 3.24^{c}	200 ± 1.62^{a}	88 ± 2.52^{a}	1350 ± 9.65^{a}	10.02 ± 2.01^{a}

Remarks: Data in the table are expressed as mean ± standard deviation of three replicates ($n = 3$), letter a, b, c, etc. resembles significant differences between treatments at $p \leq 0.05$ by Duncan's Multiple Range Test

as a promising antifungal agent and can successfully combat seed-borne pathogens of wheat. In this context, it is important to better understand the nanoparticle's structural configuration. The UV–vis spectral peak obtained for NC and Ag-NC suggested the formation of desired nanoparticles, as it corresponds to the previous work done by Kalaivani et al. (2018); Gohary et al. (2021), and Mirda et al. (2021). It is believed that the smaller is the particle size, the easier its penetration into the biological membrane (Labhasetwar et al. 1997; Bhattarai et al. 2006). The range of particle size distribution of NC and Ag-NC acquired through HRTEM analysis strongly tally with the results published in the reports of Hoang et al. (2022) and Ali et al. (2011). Various research supports the idea that particle size within 500 nm is efficient for ingression into the fungal cell membrane with ease (Desai, 2016). Irregular to spherical aggregative topography of both the nanoparticles obtained through FESEM analysis strongly coincides with the results obtained in the previous reports (Murugan et al. 2017; Sen et al. 2020). Furthermore, EDXS analysis also confirmed the presence of Ag^+ in Ag-NC, which could be regarded as a metallic nano-composite (Mirda et al. 2021).

In the present study, *A. flavus* and *A. niger* showed high frequency in the screened seeds, and treatment of seeds with NC and Ag-NC resulted in their remarkable reduction. Various workers have experimentally proved the high occurrence of *Aspergillus* spp. as a dominant seed-borne pathogen in stored wheat (Baka 2014; Mohmed et al. 2019; Kumar et al. 2023). Examination on percent inhibition of radial growth (PIRG) discloses complete termination of radial mycelial growth of *A. flavus* and *A. niger* on the application of 0.5 mg/mL of Ag-NC on PDA plate. Inversely, at the highest used dosage (0.5 mg/mL) of NC, both *A. flavus* and *A. niger* showed only 22.3% and 59.12% of PIRG, which infers NC to be barely efficient as an antifungal agent in comparison to Ag-NC. Thus, Ag-NC exhibited potentially more antifungal properties in contrast to NC. Various other groups of researchers also agreed that Ag-NC is a more potent antifungal agent than NC due to the add-on competence of Ag^+ ion (Dananjaya et al. 2017). The promotive impact of metal-dopped nanoparticles or chitosan-metal conjugates on various seed-borne pathogens has already been established by several researchers (Sangeetha and Sudha, 2019; Encinas et al. 2020). With the gradual rise in the dosimetry of Ag-NC on the PDA plate, the diameter of the radial colony of *A. flavus* and *A. niger* was observed to be decreased. This gradual decrease in the colony diameter confirms the dose-dependent functioning of metal-derived nanoparticles (Tareq et al. 2018). Several groups of workers reported the fungicidal activity of Ag^+-chitosan nanoparticles at a maximum of 1 mg/mL concentration against *Aspergillus* spp. and other related seed-borne pathogens (Kaur et al. 2012; Kalaivani et al. 2018; Shehabeldine et al. 2022). Whereas, our study demonstrated that Ag^+ complexed with chitosan nanoparticles delivers complete depletion of both *A. flavus* and *A. niger* only at 0.5 mg/mL concentration. An in-depth review on the implementation of Ag^+ ion on chitosan meshwork expresses a promotive inhibitory effect not only against a large number of seed-borne pathogens but also against several phytopathogens. It is believed that the amino group of the polycationic chitosan coalesce with the negatively charged fungal cell components, thereby suppressing the fungal ramification by chelation and inhibiting fungal enzymes (Shehabeldine et al. 2022).

The consequence of different concentrations of NC and Ag-NC on lipid peroxidation of *A. flavus* and *A. niger* was estimated by determining the MDA content generated due to oxidative stress on the application of the aforesaid nanoparticles. It is claimed that the polyunsaturated fatty acids (PUFA) residing in the fungal membrane containing methylene (-CH_2-) group is critically affected by ROS produced as a result of lipid peroxidation of the pathogens (Kalagatur et al. 2018). Our investigation reveals the generation of high MDA content in Ag-NC-treated fungal systems in comparison to NC treatment. The obtained results are in agreement with the previously performed works suggesting the successful generation of MDA by Ag-NC and some other metallic nano chitosan in variedly tested pathogenic organisms (Farooq et al. 2022).

The level of intensity of fluorescence generated in the tested seed-borne pathogens is directly equivalent to the degree of ROS produced due to oxidative stress for the exposure nanoparticles (LeBel et al. 1992; Kumar et al. 2016). Our experiment clearly concludes the fact that metal-derived nanoparticles can generate preferably more ROS than their bulk analogues (Li et al. 2012). In accordance with this, our current investigation also displayed maximum fluorescence intensity in Ag-NC-treated mycelium as well as in the sporangium of *A. flavus* and *A. niger*. The treatment of NC at the same dosage on *A. flavus* and *A. niger* does not satisfactorily generates oxidative stress. It is known that -conjugated nanoparticles can successfully uplift the generation of high intensity of oxidative stress, disrupting fungal membrane integrity. An illustration revealed that uplifted ROS content leads to an imbalanced level of antioxidants in the fungal cell surplus, which results in the release of cytochrome C, followed by cell apoptosis (Kalagatur et al. 2018). The input of Ag^+ ion into the chitosan network successfully proved the emission of high levels of fluorescence in some of the previously tested pathogens that can tally with our study (Dananjaya et al. 2017).

The application of polycationic chitosan, in addition to super positive Ag^+ ions, results in the binding of the same to the negatively charged cellular components of the pathogens. Our outcome was compatible with the reports suggested by Alghuthaymi et al. (2020) where Ag^+-chitosan nanocomposite produced defined damages on the spore membrane of another seed-borne pathogen, *Penicillium expansum* but at a slightly higher concentration of 0.9 mg/mL. It was endorsed in some of the published works that nanoparticles comprised of metal lead to the docking of metal ions on the surface of pathogenic organisms, leading to the loss of linearity of the spores and the formation of spore aggregates (Alghuthaymi et al. 2020). From the above experiments, it can be concluded that the chitosan-Ag^+ duo is predominantly successful in imparting fungicidal activity by controlling the growth of seed-borne pathogens.

Moreover, our study also aimed to investigate the plant growth-promoting criteria of chitosan-derived nanoparticles. Experiments conducted in vivo revealed that 0.5 mg/mL of Ag-NC can provide maximum protection against infection of seed-borne pathogens on wheat seeds through solid matrix priming. Tarakanov et al. (2023) discussed the role of metal-derived chitosan nanoparticles as a resistance elicitor and in plant growth promotion. Our results on the check of fungal load in stored wheat seeds revealed that Ag-NC priming can suppress the growth of imminent seed-borne pathogens and promote successful germination of the seeds. Enormous reports have been filed against seed-borne pathogens for executing stress on wheat seeds that lead to failure of its germination or seed abortion (Rehman et al. 2011; Hussain et al. 2013). Under this scenario, it is obligatory to establish a potential antifungal compound like Ag-NC to mitigate the detrimental effect of seed-borne pathogens from seeds.

Essential storage proteins like albumin and globulin are affected by the interference of seed-borne pathogens, resulting in the depletion of the seed quality (Kumar et al. 2023). In our study, it is experimentally proved that Ag-NC priming of stored wheat seeds enhances the levels of albumin, gliadin, glutenin, and gluten, thereby promoting seed quality. Our findings tally with the previous report that concludes the successful application of chitosan-Ag^+ nanoparticles in the elevation of total protein in monocot seeds (Anusuya and Banu, 2016). With the application of Ag-NC in our experiment, the total phenol content in the seeds raised manifold, irrespective of NC and non-primed seeds. The use of Ag-NC as a priming agent also uplifted the reduced sugar content, and the inclusion of Ag^+ ion into the plant system enhances the reduced sugar level has already proved (Siddiqi and Husen, 2022). Wheat endosperm is comprised of 70% of starch, which is one of the important by-products of gluten production (Kim and Kim 2021). Infection caused by seed-borne pathogens reduces the starch content up to 70% (Gebeyaw 2020). On exposing wheat seeds to Ag-NC priming, starch levels increased despite pathogenic interference. In the contrary, seed priming with NC does not satisfactorily promote the overall protein, reducing sugar and starch levels in wheat seeds.

Previous studies have demonstrated the fruitful application of Ag^+ chitosan nanoparticles in plant growth promotion activity. These nanocomposites promote germination, vigour and biomass of the model plant studied (Pereira et al. 2021; Gowda and Sriram 2023). Similar results were also attributed to our study, showing a high seed germination percentage in the set of seeds primed with Ag-NC followed by NC. The MGT taken by the seeds primed with Ag-NC is comparatively less than the MGT required by non-primed seeds to germinate. GSTI of the germinating wheat seedlings affirmed that Ag-NC incites maximum pathogenic stress tolerance capacity by accelerating seed germination percentage, promoting plant height, and root length with healthy vigor. Stress results due to the infection of seed-borne pathogens triggering seed germination and affecting the proliferation of vigor, showing retarded growth. Seeds without any priming could not withstand pathogenic stress, resulting in failure of seed germination and spotting of fungal colonies on the seed surface. On the other hand, seeds primed with NC showed moderate stress tolerance capacity with respect to seeds primed with Ag-NC. Results obtained from our investigation denote the promotive effect of the Ag^+ ion, implemented in the chitosan network. The input of Ag^+ into the chitosan body has been proven to be significant as it induces a growth-promoting effect and has antifungal properties compared to raw chitosan (Dananjaya et al. 2017). The elevated growth promotion activity traced in our study concludes that seed priming with Ag-NC can efficiently combat seed-borne pathogens and pass the seed to a successful germination regime.

Data for the cytotoxicity assay does not portray any toxic effect, with the increased dosimetry of both NC and Ag-NC at up to 1.4 mg/mL. The cytotoxicity of both NC and Ag-NC was noted from 1.5 mg/mL and beyond. The toxicity of Ag-NC on the seeded mammalian HEK293 cells was obtained due to the inclusion of metal Ag in the nanoparticle. There are also reports that nanoparticles involving Ag^+ exhibit dose-dependent phytotoxicity on plant physiology and accumulate in the soil, hampering the soil microbiota (Yan and Chen, 2019). Ag^+ nanoparticles are reported to show a phytotoxic effect on wheat seed germination, primary seminal root, coleoptile and biomass production at 10 to 40 mg/mL concentration (Lahuta et al. 2022). The threshold level of Ag^+ exposed

to living organisms should not exceed 20 µg/100 g of dry matter. The U.S. National Institute for Occupational Safety and Health has set the upper extent of all Ag^+ forms to be 0.01 mg/m^3 (Antsiferova et al. 2023). In our experiment, the bioactive dose of Ag-NC i.e., 0.5 mg/mL contains 1.14% of Ag^+ (analysed through EDXS), which is an approximate of 0.0057 mg/mL Ag^+ used for seed priming. The applied dosimetry of Ag^+ is extremely low and has no chance of imparting a phytotoxic effect. However, Ag^+ is considered one of the expensive metals and its large-scale application on agricultural practices could be strenuous for farmers and governments in developing countries like India. Thus, it is important to consider the cost-effectiveness of Ag^+-derived nanoparticles. Since, we have used a very low percentage of Ag^+ for configuring the nanoparticle, Ag-NC can also be regarded as a cost-effective fungicidal agent.

Conclusion

An overview of the role of nano-priming in restraining the growth of seed-borne pathogens of wheat seeds has been depicted in Fig. 7 and it has been observed that nano-priming with Ag-NC modulates the physiological and biochemical properties of the seed. Concomitantly, Ag-NC also alters the fungal spore structure, thereby arresting its further growth and preventing seedlings from contracting seed-borne diseases. On the other hand, nano priming alleviates different proteins inside the seed by mitigating the deleterious effect of seed-borne pathogens and rendering the seedlings with greater vigor and health by lowering the disease incidence.

Methods

Synthesis of NC and Ag-NC

Nanoparticles of chitosan were synthesized using an ionic gelation method using sodium tri-polyphosphate (STPP) as a cross-linker (Asgari-Targhi et al. 2018). Synthesis was carried out by using 80% N-deacetylated chitosan of low molecular grade (50–190 kDa; Sigma Aldrich). In brief, 0.1% chitosan (w/v) solubilized in 1% (v/v) aqueous acetic acid was subjected to 1 h of constant stirring followed by the dropwise addition of Sodium tripoly phosphate (STPP) solution of 1 mg/mL. The resulting opalescent solution was centrifuged at 10,000 rpm for 15 min, and the gel-like sediments harbouring the nanoparticles were diffused in distilled water and kept at 4 °C for future use.

Ag-loaded chitosan nanoparticles were developed by the chemical reduction method of Dananjaya et al. (2017) with soft modifications. 20 mM aquo-silver nitrate solution ($AgNO_3$; Sigma-Aldrich) was mixed with 0.1%

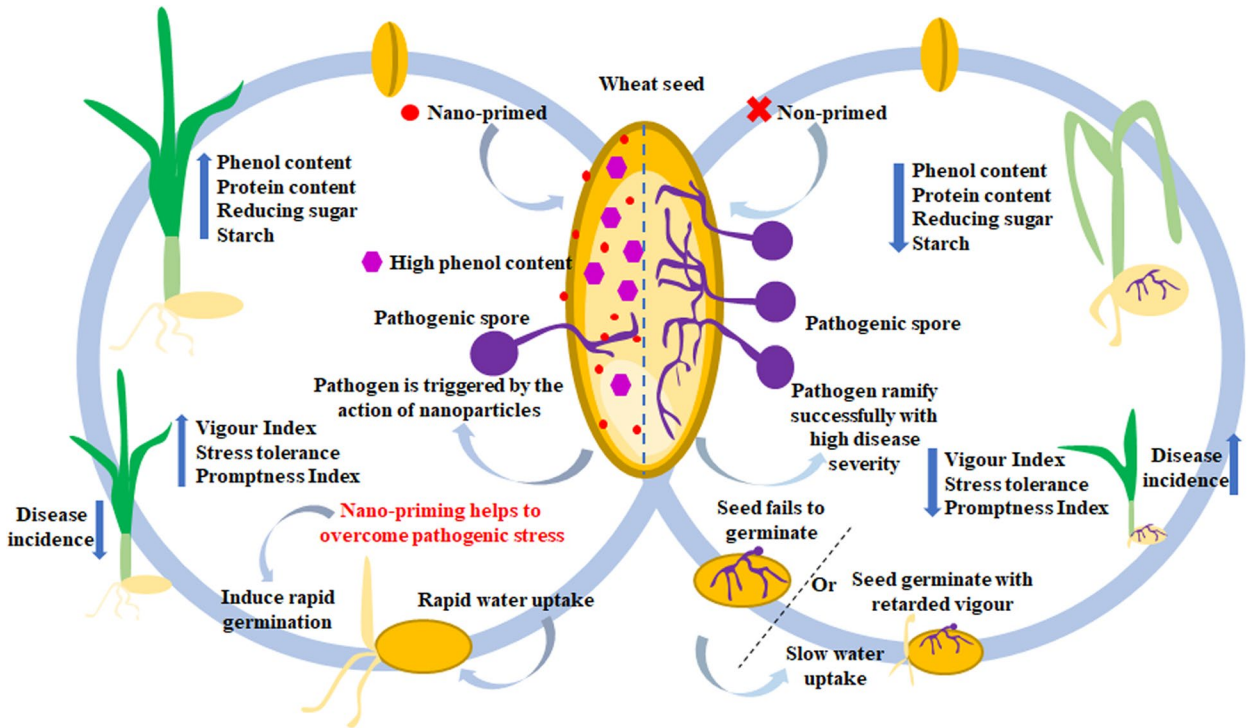

Fig. 7 Prospective role of nano-priming in modulation of wheat seed physiological that affects the growth of seed-borne pathogens and lowering disease incidence

chitosan in 0.05:3 ratio. The solution was agitated in a magnetic stirrer for 30 min followed by the addition of 50 µL sodium borohydrite of 0.2 M imparting immediate brown colouration. The solution was allowed to undergo complete reduction through the continuous stirring of 1 h. To enable cross-linking of the chitosan molecules, STPP salt was added to the aforesaid method. Centrifugation was carried out at 10,000 rpm, collecting the pellet as particles of Ag-NC.

Characterization of NC and Ag-NC

For obtaining the spectral absorbance, NC and Ag-NC were scanned between 200–800 nm on UV–vis spectrophotometer (Aligent Technologies, Carry 100 UV–Vis). High-resolution transmission electron microscopy (HRTEM) analysis was employed to detect the morphology and structure of the nanoparticles on JEOL JEM 2100F using 200 kV of accelerating potential and 50×–1.5 M×power of magnification. The exterior topography of the nanoparticles was studied through Field emission scanning electron microscopy (FESEM); Schottky JSM-7900F, JOEL, 0.1–30 kV. Detection of elements following boron was confirmed through Energy dispersive X-ray spectrometry (EDXS), especially for Ag-NC.

Isolation of seed-borne pathogens from infected wheat seeds

Infected wheat seeds of Sonalika cultivar that had typical symptoms of seed-borne diseases were collected from wheat-growing fields and seed preservatories of North Bengal, India, for the isolation of seed-borne pathogens. Permissions were granted from the wheat growers to collect infected seeds from the fields. Seed-borne fungal pathogens were isolated through the agar plate method. Infected wheat seeds were surface sterilized and seeded on sterile Petri dishes containing autoclaved potato dextrose agar (PDA) media. The isolates were further subcultured after 7 days of incubation to obtain pure cultures. Pure cultures of all the seed-borne fungal pathogens were maintained and sent for identification in IARI (Indian Agricultural Research Institute, New Delhi, India).

Effect of NC and Ag-NC on mycelium radial growth, lipid peroxidation, ROS production, and ultra-structural changes in major seed-borne pathogens *A. flavus* and *A. niger*

Poisoned food bioassay was carried out against *A. flavus* and *A. niger* using different concentrations (0.1, 0.2, 0.3, 0.4, and 0.5 mg/mL) of NC and Ag-NC (Dananjaya et al. 2017). Precisely, an aqueous solution of each concentration of both nanoparticles was blended with 20 mL of autoclaved PDA media in such a manner that the desired concentration remained unchanged in the resultant plates. A 5 mm mycelium disc of both pathogens, excised by a sterile cork-borer, was taken as inoculum. After solidification of the media, the mycelium disc was seeded at the center of a 90 mm petri plate. Also, a plate was served to both the fungus without the treatment of any nanoparticle. Plates were made in triplicates and incubated at 28 °C for 7 days. The percentage inhibition of radial growth was calculated as follows.

$$\text{PIRG (\%)} = \frac{\text{Radial growth of colony in control plate} - \text{Radial growth of colony in treated plate}}{\text{Radial growth of colony in control plate}} \times 100$$

The quantitative estimation of lipid peroxidation of both the seed-borne pathogens on application of NC and Ag-NC was determined by the synthesis of malonaldehyde (MDA), an indicator of lipid peroxidation in the pathogens (Subban et al. 2019). Mycelial mat cultured in potato dextrose broth (PDB), treated with the aforesaid range of dosimetry of both the nanoparticles, were harvested after 7 days of incubation at 28 °C. The harvested fungal mat was washed and dried with blotting paper. The mat was homogenized with chilled sodium phosphate buffer (0.1 M, pH 7) in a ratio of 1:5. Resultant homogenate was cold centrifuged at 10,000 rpm for 12 min. 100 µL of the supernatant was added to 3 mL of thiobarbituric acid (0.335%) prepared in 10% trichloroacetic acid. The developed reaction mixture was subjected to a boiling water bath until a pink colour is observed. After cooling the mixture, spectrophotometric readings were taken at 530 nm and MDA levels were calculated using 1.56×10^5 as molar absorption co-efficient.

The generation of reactive oxygen species (ROS) in both the seed-borne pathogens upon exposure of NC and Ag-NC, was spotted by using a non-fluorescent probe-2′,7′-dichlorodihydrofluorescein diacetate (H_2DCFH-DA); purchased from Sigma Aldrich, India (Chen et al. 2020). Both the pathogens were cultured in PDB treated with 0.5 mg/mL of NC and Ag-NC for 72 h. Post incubation, the hyphae were collected from the broth, washed rigorously with phosphate buffer saline (PBS), and left suspended in the same. 40 µL of H_2DCFH-DA was added to 500 µL of the hyphal suspension under dark conditions and laid for 2 h at 28 °C with sudden shaking at regular intervals. The production of ROS was spotted visually under a fluorescence microscope (Nikon Eclipse E200,

Nikon, Tokyo, Japan) using an excitation filter at 485 nm and an emission filter at 525 nm.

The morphological changes in the spore membrane of both the seed-borne pathogens at the ultra-structural level were diagnosed under a scanning electron microscope (SEM) (JSM-IT 100; JEOL). The spores cultured in PDB for 72 h, treated with 0.5 mg/mL of NC and Ag-NC were pre-treated with chemical fixatives before observation under SEM, as prescribed by Babu et al. (2018).

Effect of seed nano-priming on fungal load

Stored wheat seeds of Sonalika cultivar, collected from the regional sub-station of National Seed Corporation of India Ltd., were surface sterilized and primed with 0.5 mg/mL of NC and Ag-NC as defense elicitors, using Celite (O_2Si; Himedia) as an inert solid matrix agent. Seeds and celite were taken in 1:1 proportion, followed by maintaining 10% matrix moisture with the priming agent used. Seeds were primed for 24 h in air-tight zipper bags and held undisturbed in a seed germinator (REMI) at 22 ± 2 °C. After 24 h, the celite was sieved off, and seeds were collected (Sen et al. 2020). Four primed seeds from both treatments were placed in each petri plate containing 20 mL sterilized PDA media. A plate containing non-primed seeds was used as a control. Every treatment was made upon three replicates. Plates were incubated at 22 °C for three days. Colony Forming Units (CFU) were recorded, and the fungal load was calculated by the following equation (Andualem et al. 2019).

$$N = \frac{5a * 10000}{bt}$$

where, N = fungal CFU/m^3; a = number of colonies per Petri dish; b = surface area of dish (cm^2); t = exposure time (min).

Effect of seed nano-priming on seed quality, germination and disease incidence of wheat seeds

Estimation of total reducing sugar in the nano-primed seeds were carried out through the DNSA method suggested by Miller (1959) using maltose as standard. Total glutenin, gliadin, globulin, and albumin present in the nano-primed seeds were estimated by method Zhao et al. (2021) with minor modifications. Profiling of total seed protein were conducted through SDS-PAGE (Zhao et al. 2021). For starch estimation, 50 mg of nano-primed seeds were homogenized in 80% ethanol and subjected to 80 °C for 1 h. The starch is extracted with 52% perchloric acid in a hot, acidic medium. Colorimetric observations were recorded at 620 nm after the addition of Anthrone reagent (Clegg 1956). Changes in the total phenol content after nano-priming in the wheat seeds were estimated using the Folin-Ciocalteu method using the gallic acid standard as prescribed by Malick and Singh (1980).

Stored wheat seeds were primed with 0.5 mg/mL of NC and Ag-NC and germinated by following standard blotter paper method in sterile petri plates for seven days at 22 ± 2 °C (Khan et al. 2023). Each plate was seeded with 30 seeds. Petri plates were fixed with three layers of soaked blotter papers. Parameters such as seed germination (SG), mean germination time (MGT), germination stress tolerance index (GSTI), promptness index (PI), and vigour index (VI) were studied (Abdul- Baki & Anderson, 1972; Sen et al. 2020) in NC and Ag-NC primed seeds.

A number of 30 stored wheat seeds were nano-primed with the aforesaid dosimetry of NC and Ag-NC and allowed to germinate for seven days in sterile petri plates at 22 ± 2 °C by following the standard blotter method, as mentioned above. Percentage of disease incidence was evaluated as follows (Guha and Sindhu 2011):

$$\text{Disease incidence (DI)\%} = \frac{\text{Total no. of diseased or ungerminated seeds}}{\text{Total no. of seeds placed}} \times 100$$

Determination of cytotoxicity of NC and Ag-NC

The mammalian kidney cell line (HEK293) was purchased from the National Centre for Cell Science (NCCS), Pune, India. The cytotoxicity of both nanoparticles was determined by MTT (3-(4,5-dimethylthiazol-2-yl)-2,5-diphenyltetrazolium bromide) assay (Mosmann 1983; Denizot & Lang, 1986). Briefly, a rapidly multiplying mammalian kidney cell line was placed in 96 well microtiter plate using 6×10^3 cells/well. The wells were maintained in 5% CO_2 using DMEM (Dulbecco's Modified Eagle Medium) Ham F-12 cell culture medium at 37 °C. After 24 h of proliferation, wells were treated with different concentrations (0.1–2 mg/mL) of NC and Ag-NC in triplicate. After 24 h of further incubation, the culture media was aspirated, followed by the addition of 10 µL MTT dissolved in 1 × PBS in each well and laid for 3 h. Before recording the absorbance in the ELISA reader at 620 nm, 50 µL of isopropanol was added to each well with occasional shaking for 10 min.

$$\text{Cytotoxicity \%} = \frac{\text{Mean optical density of untreated cells} - \text{Mean optical density of treated cells}}{\text{Mean optical density of untreated cells}} \times 100$$

Statistical analysis

The results obtained from the experiments conducted are the mean of five different observations with standard deviation (SD) (Mean ± SD). Statistical differences were investigated by using Duncan's Multiple Range Test (DMRT) at $p \leq 0.05$ (DSAASTAT ver. 1.022); treatments differing significantly are represented by letters a, b, c, etc.

Abbreviations

EDXS	Energy dispersive X-ray spectrometry
FESEM	Field emission scanning electron microscopy
GSTI	Germination stress tolerance index
HEK	Human embryonic kidney
HRTEM	High-resolution transmission electron microscopy
kDa	Kilo Dalton
kV	Kilo volt
MDA	Malonaldehyde
MGT	Mean germination time
SDS-PAGE	Sodium dodecyl sulphate poly acrylamide gel electrophoresis
VI	Vigour index

Supplementary Information

The online version contains supplementary material available at https://doi.org/10.1186/s42483-024-00260-x.

Additional file 1: Figure S1. Isolation of seed-borne pathogens from infected wheat seeds; microscopic observation of *A. flavus* and *A. niger*.

Additional file 2: Figure S2. Growth of *A. flavus* and *A. niger* under exposure of $AgNO_3$served as positive control effect of different concentrations of Ag, Ag-NC, and $AgNO_3$ on colony diameter of *A. flavus* and *A. niger*.

Additional file 3: Figure S3. Comparison of cytotoxicity of NC and Ag-NC on mammalian kidney HEK293 cells. Cellular toxicity was evaluated based on the percentage of cytotoxicity with different concentrations of NC and Ag-NC (0.1–2 mg/mL). Data are expressed as the mean ± standard deviation (*n*=3).

Acknowledgements

The authors are highly grateful to the University of North Bengal for providing the necessary research support. The authors are also thankful to National Seeds Corp. Ltd., New Delhi, SAIF-IIT Bombay, CIF-LPU (India) for their assistance and co-operation. PM acknowledges the DST-FIST facility, Department of Botany (Sanc. No. SR/FST/LS-I/2021/900) for all instrumentation facility.

Authors' contributions

PM, CC, and PM conceptualized the work.; DC, DD, AK, and AK performed the research. DC carried out all the formal analysis, analysed data, prepared the original draft. PM and DC wrote and edited the entire manuscript.

Funding

All authors would like to thank the University Grant Commission (Government of India) for providing UGC-NET SRF Fellowship (672/CSIRNET JUNE 2019).

Availability of data and materials

Research data will be shared on request.

Declarations

Ethics approval and consent to participate

Not applicable.

Consent for publication

Not applicable.

Competing interests

The authors declare no competing interests.

Received: 17 September 2023 Accepted: 26 May 2024
Published online: 09 August 2024

References

Abdul-Baki AA, Anderson JD. Physiological and biochemical deterioration of seeds. Seed Biology. 1972;2:283–315.

Alghuthaymi MA, Abd-Elsalam KA, Shami A, Said-Galive E, Shtykova EV, Naumkin AV. Silver/Chitosan nanocomposites: Preparation and characterization and their fungicidal activity against dairy cattle toxicosis *Penicillium expansum*. J Fungi. 2020;6(2):51.

Ali SW, Rajendran S, Joshi M. Synthesis and characterization of chitosan and silver loaded chitosan nanoparticles for bioactive polyester. Carbohydr Polym. 2011;83(2):438–46.

Ali MA, Shahzadi M, Zahoor A, Dababat AA, Toktay H, Bakhsh A, Nawaz MA, Li H. Resistance to cereal cyst nematodes in wheat and barley: an emphasis on classical and modern approaches. Int J Mol Sci. 2019;20(2):432.

Andualem Z, Gizaw Z, Dagne H. Indoor culturable fungal load and associated factors among public primary school classrooms in Gondar City, Northwest Ethiopia, 2018: a cross-sectional study. Ethiopian J Health Sci. 2019;29(5):623-30.

Antonoglou O, Moustaka J, Adamakis ID, Sperdouli I, Pantazaki AA, Moustakas M, Dendrinou-Samara C. Nanobrass CuZn nanoparticles as foliar spray nonphytotoxic fungicides. ACS Appl Mater Interfaces. 2018;10(5):4450–61.

Antsiferova AA, Kopaeva MY, Kochkin VN, Reshetnikov AA, Kashkarov PK. Neurotoxicity of Silver Nanoparticles and Non-Linear Development of Adaptive Homeostasis with Age. Micromachines. 2023;14(5):984. https://doi.org/10.3390/mi14050984.

Anusuya S, Banu KN. Silver-chitosan nanoparticles induced biochemical variations of chickpea (Cicer arietinum L). Biocatal Agric Biotechnol. 2016;8:39–44.

Ardean C, Davidescu CM, Nemeş NS, Negrea A, Ciopec M, Duteanu N, Negrea P, Duda-Seiman D, Musta V. Factors influencing the antibacterial activity of chitosan and chitosan modified by functionalization. Int J Mol Sci. 2021;22(14):7449.

Asgari-Targhi G, Iranbakhsh A, Ardebili ZO. Potential benefits and phytotoxicity of bulk and nano-chitosan on the growth, morphogenesis, physiology, and micropropagation of *Capsicum annuum*. Plant Physiol Biochem. 2018;127:393–402.

Baka ZA. Plant extract control of the fungi associated with different Egyptian wheat cultivars grains. J Plant Prot Res. 2014;54(3):231–7.

Banerjee A, Sarkar A, Acharya K, Chakraborty N. Nanotechnology: an emerging hope in crop improvement. Lett Appl NanoBioScience. 2021;10(4):2784–803.

Bhattarai N, Ramay HR, Chou SH, Zhang M. Chitosan and lactic acid-grafted chitosan nanoparticles as carriers for prolonged drug delivery. International J Nanomed. 2006;1(2):181–7.

Chen J, Wu L, Lu M, Lu S, Li Z, Ding W. Comparative study on the fungicidal activity of metallic MgO nanoparticles and macroscale MgO against soilborne fungal phytopathogens. Front Microbiol. 2020;11:511894.
Choudhary P. Harmful Effects of Fungicides-Current Status, New Delhi Publishers. 2018.
Clegg KM. The application of the anthrone reagent to the estimation of starch in cereals. J Sci Food and Agric. 1956;7(1):40–4.
Dananjaya SH, Erandani WK, Kim CH, Nikapitiya C, Lee J, De Zoysa M. Comparative study on antifungal activities of chitosan nanoparticles and chitosan silver nano composites against *Fusarium oxysporum* species complex. Int J Biol Macromol. 2017;105:478–88.
Denizot F, Lang R. Rapid colorimetric assay for cell growth and survival: modifications to the tetrazolium dye procedure giving improved sensitivity and reliability. J Immunol Methods. 1986;89(2):271–7.
Desai KG. Chitosan nanoparticles prepared by ionotropic gelation: An overview of recent advances. Crit Rev Ther Drug Carr Syst. 2016;33(2):107-58.
E EG, EL, Gohary, M S, Farag, EL-Sayed A, R R, Khattab, M D, Mahmoud. Insecticidal activity and biochemical study of the clove oil (Syzygium aromaticum) nano-formulation on Culex pipiens L (diptera Culicidae). Egypt J Aquat Res. 2021;25(1):227–39.
Encinas D, Carvajal FA, Calderon AA, et al. Silver nanoparticles coated with chitosan against *Fusarium oxysporum* causing the tomato wilt. Biotecnia. 2020;22(3):73–80.
Eskikaya O, Özdemir S, Gonca S, Dizge N, Balakrishnan D, Shaik F, Senthilkumar N. A comparative study of iron nanoflower and nanocube in terms of antibacterial properties. Appl Nanosci. 2023;13(8):5421–33.
do Espirito Santo Pereira A, Caixeta Oliveira H, Fernandes Fraceto L, Santaella C. Nanotechnology potential in seed priming for sustainable agriculture. Nanomaterials. 2021;11(2):267.
Farooq T, Nisa ZU, Hameed A, Ahmed T, Hameed A. Priming with copper-chitosan nanoparticles elicit tolerance against PEG-induced hyperosmotic stress and salinity in wheat. BMC Chemistry. 2022;16(1):23.
Gebeyaw M. Review on: Impact of seed-borne pathogens on seed quality. Am J Plant Biol. 2020;5:77–81.
Gowda S, Sriram S. Green synthesis of chitosan silver nanocomposites and their antifungal activity against *Colletotrichum truncatum* causing anthracnose in chillies. Plant Nano Biol. 2023;5:100041.
Hans ML, Lowman AM. Biodegradable nanoparticles for drug delivery and targeting. Curr Opin Solid State Mater Sci. 2002;6(4):319–27.
Hoang NH, Le Thanh T, Sangpueak R, Treekoon J, Saengchan C, Thepbandit W, Papathoti NK, Kamkaew A, Buensanteai N. Chitosan nanoparticles-based ionic gelation method: a promising candidate for plant disease management. Polymers. 2022;14(4):662.
Hussain M, Ghazanfar MU, Hamid MI, Raza M. Seed borne mycoflora of some commercial wheat (Triticum aestivum L.) cultivars in Punjab. Pakistan Int J Phytopathol. 2013;2(2):97–101.
Ibrahim E, Zhang M, Zhang Y, Hossain A, Qiu W, Chen Y, Wang Y, Wu W, Sun G, Li B. Green-synthesization of silver nanoparticles using endophytic bacteria isolated from garlic and its antifungal activity against wheat *Fusarium* head blight pathogen *Fusarium graminearum*. Nanomaterials. 2020;10(2):219.
Il'Ina AV, Shagdarova BT, Lun'Kov AP, Kulikov SN, Varlamov VP. In vitro antifungal activity of metal complexes of a quaternized chitosan derivative with copper ions. Microbiology. 2017;86:590–5.
Islam MS, Sarker MN, Ali MA. Effect of seed borne fungi on germinating wheat seed and their treatment with chemicals. Int J Nat Soc Sci. 2015;2(1):28–32.
Jiang W, Tao T, Liao Z. Removal of heavy metal from contaminated soil with chelating agents. Open J Soil Sci. 2011;1(2):71–7.
Kadege E, Lyimo HJ. Prevalence and control of wheat (Triticum aestivum L.) seed borne fungi in farmer-saved seeds. Arch Phytopathol Plant Prot. 2015;48(7):601–10.
Kalagatur NK, Nirmal Ghosh OS, Sundararaj N, Mudili V. Antifungal activity of chitosan nanoparticles encapsulated with *Cymbopogon martinii* essential oil on plant pathogenic fungi *Fusarium graminearum*. Front Pharmacol. 2018;9:356156.
Kalaivani R, Maruthupandy M, Muneeswaran T, Beevi AH, Anand M, Ramakritinan CM, Kumaraguru AK. Synthesis of chitosan mediated silver nanoparticles (Ag NPs) for potential antimicrobial applications. Front Lab Med. 2018;2:30–5.
Kale SK, Parishwad GV, Patil AS. Emerging agriculture applications of silver nanoparticles. ES Food & Agroforestry. 2021;3:17–22.
Kaur P, Thakur R, Choudhary A. An in vitro study of the antifungal activity of silver/chitosan nanoformulations against important seed borne pathogens. Int J Sci Technol Res. 2012;1(6):83–6.
Kaur P, Thakur R, Barnela M, Chopra M, Manuja A, Chaudhury A. Synthesis, characterization and in vitro evaluation of cytotoxicity and antimicrobial activity of chitosan–metal nanocomposites. J Chem Technol Biotechnol. 2015;90(5):867–73.
Khan AM, Khan M, Salman HM, Ghazali HM, Ali RI, Hussain M, Yousaf MM, Hafeez Z, Khawja MS, Alharbi SA, Alfarraj S. Detection of seed-borne fungal pathogens associated with wheat (Triticum aestivum L.) seeds collected from farmer fields and grain market. Journal of King Saud University-Science. 2023;35(4):102590.
Kim KH, Kim JY. Understanding wheat starch metabolism in properties, environmental stress condition, and molecular approaches for value-added utilization. Plants. 2021;10(11):2282.
Kong M, Chen XG, Xing K, Park HJ. Antimicrobial properties of chitosan and mode of action: a state of the art review. Int J Food Microbiol. 2010;144(1):51–63.
Kumar KN, Venkataramana M, Allen JA, Chandranayaka S, Murali HS, Batra HV. Role of Curcuma longa L. essential oil in controlling the growth and zearalenone production of Fusarium graminearum. LWT-Food Sci and Technol. 2016;69:522–8.
Kumar N, Khurana SP, Pandey VN. Deciphering of seed Health of common food grains (wheat, rice) of North Eastern UP and Gurgaon Haryana, India. Sci Rep. 2023;13(1):8480.
Kumari M, Pandey S, Bhattacharya A, Mishra A, Nautiyal CS. Protective role of biosynthesized silver nanoparticles against early blight disease in *Solanum lycopersicum*. Plant Physiol Biochem. 2017;121:216–25.
Labhasetwar V, Song C, Levy RJ. Nanoparticle drug delivery system for restenosis. Adv Drug Del Rev. 1997;24(1):63–85.
Lahuta LB, Szablińska-Piernik J, Głowacka K, Stałanowska K, Railean-Plugaru V, Horbowicz M, et al. The Effect of Bio-Synthesized Silver Nanoparticles on Germination Early Seedling Development and Metabolome of Wheat (*Triticum aestivum* L.). Molecules. 2022;27(7):2303. https://doi.org/10.3390/molecules27072303.
LeBel CP, Ischiropoulos H, Bondy SC. Evaluation of the probe 2', 7'-dichlorofluorescin as an indicator of reactive oxygen species formation and oxidative stress. Chem Res Toxicol. 1992;5(2):227–31.
Li Y, Zhang W, Niu J, Chen Y. Mechanism of photogenerated reactive oxygen species and correlation with the antibacterial properties of engineered metal-oxide nanoparticles. ACS Nano. 2012;6(6):5164–73.
Liu W, Qin Y, Liu S, Xing R, Yu H, Chen X, Li K, Li P. Synthesis of C-coordinated O-carboxymethyl chitosan metal complexes and evaluation of their antifungal activity. Sci Rep. 2018;8(1):4845.
Mahakham W, Sarmah AK, Maensiri S, Theerakulpisut P. Nanopriming technology for enhancing germination and starch metabolism of aged rice seeds using phytosynthesized silver nanoparticles. Sci Rep. 2017;7(1):8263.
Majumder D, Rajesh T, Suting EG, Debbarma A. Detection of seed borne pathogens in wheat: recent trends. Aust J Crop Sci. 2013;7(4):500–7.
Malerba M, Cerana R. Chitosan effects on plant systems. Int J Mol Sci. 2016;17(7):996.
Malick CP, Singh MB. Plant Enzymology and Histo enzymology. 1st ed. New Delhi: Kalyani Publishers; 1980.
Mansoor S, Zahoor I, Baba TR, Padder SA, Bhat ZA, Koul AM, Jiang L. Fabrication of silver nanoparticles against fungal pathogens. Front Nanotechnol. 2021;3:679358.
Martín I, Gálvez L, Guasch L, Palmero D. Fungal pathogens and seed storage in the dry state. Plants. 2022;11(22):3167.
Mehboob S, Rehman A, Ali S, Idrees M, Zaidi SH. Detection of wheat seed mycoflora with special reference to Drechslera sorokiniana. Pak J Phytopathol. 2015;27(1):21–6.
Miller GL. Use of dinitrosalicylic acid reagent for determination of reducing sugar. Anal Chem. 1959;31(3):426–8.
Mirda E, Idroes R, Khairan K, Tallei TE, Ramli M, Earlia N, Maulana A, Idroes GM, Muslem M, Jalil Z. Synthesis of chitosan-silver nanoparticle composite spheres and their antimicrobial activities. Polymers. 2021;13(22):3990.
Mohmed AA, Elsiddig MA, Haroun NE. Isolation of seed borne pathogens associated with some cereal grains in Khartoum state (Sudan). Int J Sci Res Pub. 2019;9(4):110–3.

Mosmann T. Rapid colorimetric assay for cellular growth and survival: application to proliferation and cytotoxicity assays. J Immunol Methods. 1983;65(1–2):55–63.
Murugan K, Jaganathan A, Suresh U, Rajaganesh R, Jayasanthini S, Higuchi A, Kumar S, Benelli G. Towards bio-encapsulation of chitosan-silver nanocomplex? Impact on malaria mosquito vectors, human breast adenocarcinoma cells (MCF-7) and behavioral traits of non-target fishes. J Clust Sci. 2017;28:529–50.
Nagaraja SK, Kumar RS, Chakraborty B, Hiremath H, Almansour AI, Perumal K, Gunagambhire PV, Nayaka S. Biomimetic synthesis of silver nanoparticles using Cucumis sativus var. hardwickii fruit extract and their characterizations, anticancer potential and apoptosis studies against Pa-1 (Human ovarian teratocarcinoma) cell line via flow cytometry. Appl Nanosci. 2023;13(4):3073–84.
Nguyen TD, Nguyen HT, Thi NT, Phung HT, Trinh GN. Antifungal activity against plant pathogens of purely microwave-assisted copper nanoparticles using Citrus grandis peel. Appl Nanosci. 2023;13(8):5697–709.
Pincus LN, Petrović PV, Gonzalez IS, Stavitski E, Fishman ZS, Rudel HE, Anastas PT, Zimmerman JB. Selective adsorption of arsenic over phosphate by transition metal cross-linked chitosan. Chem Eng J. 2021;412:128582.
Pivarčiová L, Rosskopfová O, Galamboš M, Rajec P. Sorption of nickel on chitosan. J Radioanal Nucl Chem. 2014;300:361–6.
Qiang FX, Fang LX, Sheng Y, Qing FG, Pu WT. Anti-*Aspergillus niger* activity of metal/chitosan complexes. Food Sci. 2011;32:152–5.
Rao GS, Narayana SL, Bhadraiah B, Manoharachary C. Biochemical changes due to fungal infestation in stored seeds of some vegetable crops. Indian Phytopathol. 2014;67:159–63.
Raza M, Hussain M, Ghazanfer MU. Characterization and pathogenicity of *Biplolaris sorokiniana* caused spot blotch of wheat in Pakistan. FUUAST J Biol. 2014;4(1):97–100.
Rehman A, Sultana K, Minhas N, Gulfraz M, Raja GK, Anwar Z. Study of most prevalent wheat seed-borne mycoflora and its effect on seed nutritional value. Afr J Microbiol Res. 2011;5(25):4328–37.
Sadak MS. Impact of silver nanoparticles on plant growth, some biochemical aspects, and yield of fenugreek plant (*Trigonella foenum-graecum*). Bull Nat Res Cent. 2019;43(1):1–6.
Sahu GK, Sindhu SS. Disease control and plant growth promotion of green gram by siderophore producing *Pseudomonas* sp. Res J Microbiol. 2011;6(10):735.
Sangeetha K, Sudha PN. Antimicrobial characterization of silver nanoparticle-coated polyvinyl alcohol/nanochitosan surface by "touch test" method. J Indian Chem Soc. 2019;96(1):176–9.
Santiago TR, Bonatto CC, Rossato M, Lopes CA, Lopes CA, G Mizubuti ES, Silva LP. Green synthesis of silver nanoparticles using tomato leaf extract and their entrapment in chitosan nanoparticles to control bacterial wilt. J Sci Food Agric. 2019;99(9):4248–59.
Sarkar A, Acharya K. Chitosan: A promising candidate for sustainable agriculture. In: Chourasia HK, Acharya K, Singh VK, editors. Precision Agriculture and Sustainable Crop Production. India: Today and Tomorrow's Printers and Publishers; 2020. p. 391–407.
Sarwar M. Pattern of damage by rodent (Rodentia: Muridae) pests in wheat in conjunction with their comparative densities throughout growth phase of crop. Int J Environ Sci. 2015;3(4):159–66.
Sathiyabama M, Charles RE. Fungal cell wall polymer based nanoparticles in protection of tomato plants from wilt disease caused by Fusarium oxysporum f. sp. lycopersici. Carbohydr Polym. 2015;133:400–7.
Sathiyabama M, Parthasarathy R. Biological preparation of chitosan nanoparticles and its *in vitro* antifungal efficacy against some phytopathogenic fungi. Carbohydr Polym. 2016;151:321–5.
Sen SK, Chouhan D, Das D, Ghosh R, Mandal P. Improvisation of salinity stress response in mung bean through solid matrix priming with normal and nano-sized chitosan. Int J Biol Macromol. 2020;145:108–23.
Sharma J, Singh VK, Kumar A, Shankarayan R, Mallubhotla S. Role of Silver Nanoparticles in Treatment of Plant Diseases. In: Patra J, Das G, Shin HS (eds). Microbial Biotechnology. Singapore: Springer; 2018. https://doi.org/10.1007/978-981-10-7140-9_20.
Shehabeldine AM, Salem SS, Ali OM, Abd-Elsalam KA, Elkady FM, Hashem AH. Multifunctional silver nanoparticles based on chitosan: Antibacterial, antibiofilm, antifungal, antioxidant, and wound-healing activities. J Fungi. 2022;8(6):612.
Siddiqi KS, Husen A. Plant response to silver nanoparticles: a critical review. Crit Rev Biotechnol. 2022;42(7):973–90.
Subban K, Subramani R, Srinivasan VP, Johnpaul M, Chelliah J. Salicylic acid as an effective elicitor for improved taxol production in endophytic fungus *Pestalotiopsis microspora*. PLoS ONE. 2019;14(2):e0212736.
Tahmasebi A, Roach T, Shin SY, Lee CW. Fusarium solani infection disrupts metabolism during the germination of roselle (Hibiscus sabdariffa L.) seeds. Front Plant Sci. 2023;14:1225426.
Tarakanov R, Shagdarova B, Lyalina T, Zhuikova Y, Il'ina A, Dzhalilov F, Varlamov V. Protective properties of copper-loaded chitosan nanoparticles against soybean pathogens Pseudomonas savastanoi pv. glycinea and Curtobacterium flaccumfaciens pv. flaccumfaciens. Polymers. 2023;15(5):1100.
Tareq FK, Fayzunnesa M, Kabir MS, Nuzat M. RETRACTED: Evaluation of dose dependent antimicrobial activity of self-assembled chitosan, nano silver and chitosan-nano silver composite against several pathogens. 2018.
Tripathi DK, Tripathi AS, Singh S, Singh Y, Vishwakarma K, Yadav G, Sharma S, Singh VK, Mishra RK, Upadhyay RG. Uptake, accumulation and toxicity of silver nanoparticle in autotrophic plants, and heterotrophic microbes: a concentric review. Front Microbiol. 2017;8:07.
Venkatesh Babu G, Perumal P, Muthu S, Pichai S, Sankar Narayan K, Malairaj S. Enhanced method for high spatial resolution surface imaging and analysis of fungal spores using scanning electron microscopy. Sci Rep. 2018;8(1):16278.
Wang X, Du Y, Fan L, Liu H, Hu Y. Chitosan-metal complexes as antimicrobial agent: Synthesis, characterization and Structure-activity study. Poly Bull. 2005;55:105–13.
Wang LS, Wang CY, Yang CH, Hsieh CL, Chen SY, Shen CY, Wang JJ, Huang KS. Synthesis and anti-fungal effect of silver nanoparticles–chitosan composite particles. Int J Nanomed. 2015;10:2685–96.
Yan A, Chen Z. Impacts of silver nanoparticles on plants: A Focus on the Phytotoxicity and Underlying Mechanism. Int J Mol Sci. 2019;20(5):1003.
Yanat M, Schroën K. Preparation methods and applications of chitosan nanoparticles; with an outlook toward reinforcement of biodegradable packaging. Reactive Func Poly. 2021;161:104849.
Zhao J, Li Z, Khan MU, Gao X, Yu M, Gao H, Li Y, Zhang H, Dasanayaka BP, Lin H. Extraction of total wheat (*Triticum aestivum*) protein fractions and cross-reactivity of wheat allergens with other cereals. Food Chem. 2021;347:129064.